SDU
University of Southern Denmark

Digestion of surfactants does not affect their ability to inhibit P-gp-mediated transport in vitro

Rasmussen, Asbjørn Jaensch; Pedersen, Maria; Griffin, Brendan T; Holm, René; Nielsen, Carsten Uhd

Published in:
International Journal of Pharmaceutics

DOI:
10.1016/j.ijpharm.2024.124120

Publication date:
2024

Document version:
Final published version

Document license:
CC BY

Citation for pulished version (APA):
Rasmussen, A. J., Pedersen, M., Griffin, B. T., Holm, R., & Nielsen, C. U. (2024). Digestion of surfactants does not affect their ability to inhibit P-gp-mediated transport in vitro. *International Journal of Pharmaceutics*, *656*, 124120. https://doi.org/10.1016/j.ijpharm.2024.124120

Go to publication entry in University of Southern Denmark's Research Portal

Terms of use
This work is brought to you by the University of Southern Denmark.
Unless otherwise specified it has been shared according to the terms for self-archiving.
If no other license is stated, these terms apply:

- You may download this work for personal use only.
- You may not further distribute the material or use it for any profit-making activity or commercial gain
- You may freely distribute the URL identifying this open access version

If you believe that this document breaches copyright please contact us providing details and we will investigate your claim.
Please direct all enquiries to puresupport@bib.sdu.dk

Download date: 10. Jan. 2025

International Journal of Pharmaceutics 656 (2024) 124120

Contents lists available at ScienceDirect

International Journal of Pharmaceutics

journal homepage: www.elsevier.com/locate/ijpharm

Digestion of surfactants does not affect their ability to inhibit P-gp-mediated transport *in vitro*

Asbjørn Jaensch Rasmussen [a], Maria Pedersen [a], Brendan T. Griffin [b], René Holm [a], Carsten Uhd Nielsen [a,*]

[a] *Department of Physics, Chemistry and Pharmacy, University of Southern Denmark, Campusvej 55 DK-5230, Odense M, Denmark*
[b] *School of Pharmacy, University College Cork, College Road, Cork T12 YN60, Ireland*

A R T I C L E I N F O

Keywords:
P-gp
Digoxin
Surfactants
Digestion
Caco-2
MDCKII-MDR1

A B S T R A C T

While various non-ionic surfactants at low concentrations have been shown to increase the transport of P-gp substrates *in vitro*, *in vivo* studies in rats have shown that a higher surfactant concentration is needed to increase the oral absorption of e.g. the P-gp substrates digoxin and etoposide. The aim of the present study was to investigate if intestinal digestion of surfactants could be the reason for this deviation between *in vitro* and *in vivo* data. Therefore, Kolliphor EL, Brij-L23, Labrasol and polysorbate 20 were investigated for their ability to inhibit P-gp and increase digoxin absorption *in vitro*. Transport studies were performed in Caco-2 cells, while P-gp inhibition and cell viability assays were performed in MDCKII-MDR1 cells. Polysorbate 20, Kolliphor EL and Brij-L23 increased absorptive transport and decreased secretory digoxin transport in Caco-2 cells, whereas only polysorbate 20 and Brij-L23 showed P-gp inhibiting properties in the MDCKII-MDR1 cells. Polysorbate 20 and Brij-L23 were chosen for *in vitro* digestion prior to transport- or P-gp inhibiting assays. Brij-L23 was not digestible, whereas polysorbate 20 reached a degree of digestion around 40%. Neither of the two surfactants showed any significant difference in their ability to affect absorptive or secretory transport of digoxin after predigestion. Furthermore, the P-gp inhibiting effects of polysorbate 20 were not decreased significantly. In conclusion, the mechanism behind the non-ionic surfactant mediated *in vitro* P-gp inhibition seemed independent of the intestinal digestion and the results presented here did not suggest it to be the cause of the observed discrepancy between *in vitro* and *in vivo*.

1. Introduction

The intestinal permeability of certain drug substances is limited by the apically located membrane transporter P-glycoprotein (P-gp, ABCB1). P-gp mediates cellular efflux of numerous chemically unrelated drug substances, which leads to a decreased absorption and bioavailability of these substances (Leslie et al., (2005); Lin and Yamazaki (2003)). Numerous nonionic surfactants have been shown to inhibit P-gp in cell- and animal models including *in vivo* and *in situ* rodent transport studies. These pharmaceutical surfactants inhibit P-gp at relatively high concentrations in the μM range, compared to specific P-gp inhibitors with effective concentrations in the nM range (Al-Ali et al., (2019); Cornaire et al. (2004); Lo (2003); Zhang et al. (2003); Nielsen et al. (2016)). Polysorbate 20 (PS20) is among the most potent surfactant-based P-gp inhibitors investigated, with an IC_{50} value of around 11 μM (Al-Ali et al., (2018a); Al-Ali et al., (2018b); Al-Saraf et al. (2016); Gurjar et al. (2018); Lo (2003)). When the P-gp substrate digoxin was co-administered as an oral solution with 10% (w/v) (0.55 g $\cdot$ kg^{-1}) PS20 a significantly increase in the oral bioavailability of digoxin in Sprague Dawley rats from 59 to 84% was reported, and accompanied by an increase in C_{max} of 79% (Nielsen et al., (2016)). At PS20 concentrations of 10–25% (w/v) no further increase in the bioavailability of digoxin was observed and at 25% (w/v) PS20 even C_{max} tended to decrease (Nielsen et al., (2016)). In *mdr1a(−,-)* knockout Sprague Dawley rats, an increased digoxin bioavailability was seen, yet there was no effect of co-administration of 25% (w/v) PS20 in the oral solution, supporting the hypothesis, that the effects of PS20 on the *in vivo* absorption of digoxin was P-gp specific and not the result of micelle formations (Nielsen et al., (2016)). In another study using a similar approach, Al-Ali et al., (2018a) found that PS20 increased the oral absorption of etoposide in wild-type Sprague-Dawley rats. However, the bioavailability of etoposide was similar in formulations containing

* Corresponding author at: Department of Physics, Chemistry and Pharmacy, University of Southern Denmark, Campusvej 55 DK-5230, Odense M, Denmark.
E-mail address: cun@sdu.dk (C.U. Nielsen).

https://doi.org/10.1016/j.ijpharm.2024.124120
Received 8 March 2024; Received in revised form 11 April 2024; Accepted 12 April 2024
Available online 15 April 2024
0378-5173/© 2024 The Author(s). Published by Elsevier B.V. This is an open access article under the CC BY license (http://creativecommons.org/licenses/by/4.0/).

5–25% (w/v) PS20. Surprisingly, the bioavailability of etoposide in *mdr1a(−,-)* knockout Sprague-Dawley rats decreased with increasing PS20 amounts in the dosing volume. It could be shown that the absorption rate constant decreased with increasing PS20 dose, which was suggested to be due to the intraluminal formation of PS20 micelles retaining etoposide and thus reducing the free aqueous concentration available for permeation. Recently, molecular dynamics studies have shown that PS20 makes several direct interactions with the P-gp protein, including binding to the drug binding site of the transporter (Moesgaard et al., (2022)). Part of the interaction between P-gp and PS20 may be the formation of "lollipops" in the membrane, where poly(ethylene glycol) (PEG) chains of PS20 molecules tend to curl up around themselves and the fatty acid chains extending toward the core of the membrane. PS20 can move along the protein to get access to the drug binding site through the extracellular bilayer. One element of intraluminal events that was not considered in the studies by Nielsen et al. (2016) and Al-Ali et al., (2018a), was if the surfactant maintains its ability to inhibit P-gp after digestion, as PS20 is a digestible surfactant (Koehl et al., (2020)). The digestion products of PS20 are likely to be a mixture of lauric acid, myristic acid, palmitic acid and stearic acid alongside the remaining PEGyalted sorbitol moiety (Tomlinson et al., (2015)). Ali et al. (2015) designed an *in silico* method using docking simulations to screen fatty acids for P-gp inhibiting properties. They found oleic acid and stearic acid to interact with P-gp by forming hydrogen bonds inside the drug binding site of a rat P-gp model. The corresponding inhibition constants of the two fatty acids were reported to be 65.4 and 130.8 μM, respectively. In contrast to stearic acid, where no other studies have reported any P-gp inhibiting effects, Houshaymi et al. (2019) found oleic acid to increase the uptake of ivermectin, a P-gp substrate, when incorporated into complex micelles. The increased uptake of ivermectin was found both *in vitro* in Caco-2 cells and *in vivo* in wild-type mice. Furthermore, oleic acid has been shown to inhibit breast cancer resistance protein (BCRP) in Caco-2 cells. 0.5 mM oleic acid increased the transport of mitoxantrone, a BCRP substrate, without affecting the transepithelial electrical resistance (TEER) (Aspenström-Fagerlund et al., (2012)). While no readily available study has reported any effects on P-gp mediated transport by myristic or palmitic acid, lauric acid has been reported to have no effect on the accumulation of the P-gp substrate daunorubicin in P-gp overexpressing KB-C2 cells (Kitagawa et al., (2005)). The aim of the present study was thus to investigate if digestion effects the P-gp inhibitory properties of a digestible pharmaceutical surfactants. Digestible P-gp modulating surfactants such as PS20, Kolliphor EL and Labrasol was therefore studied alongside indigestible surfactant Brij-L23 (Al-Ali et al., (2019); Koehl et al. (2020)). The specific P-gp inhibition was studied using the calcein-AM assay, and transcellular permeability was studied investigating digoxin transport across Caco-2 cells in the presence of either undigested or partly digested surfactants.

2. Materials and chemicals

2.1. Chemicals

Caco-2 cells were from Deutsche Sammlung von Mikroorganismen und Zellkulturen (DSMZ) (Braunschweig, Germany) and MDCKII-MDR1 cells were from The Laboratory of Prof. Piet Borst (Amsterdam, The Netherlands). 96 well plates, tissue culture treated clear flat bottom wells, black or clear were from SPL Life Sciences (Pocheon, Gyeonggi, South Korea). 4-(2-hydroxyethyl)piperazine-1-ethanesulfonic acid (HEPES), 7.5% Sodium bicarbonate solution, Trizma® base, Kolliphor EL, calcein-AM, porcine pancreas (8x USP specification), and polysorbate 20 (PS20) were obtained from Sigma Aldrich (Burlington, MA, U.S.). Labrasol ALF was a kind gift from GatteFossé (Saint-Priest, France). DMSO was purchased from PanReac Applichem (Darmstadt, Germany). CellTiter-Glo® Luminescent Cell Viability Assay were from Promega Corporation (Madison, WI, U.S.). Hanks' balanced salt solution (HBSS), 10x, and 4-bromophenyol boronic acid were from Gibco (Thermo Fisher, Waltham, MA, U.S). Polycarbonate membrane cell culture inserts, sodium chloride, maleic acid, and calcium chloride anhydrous were purchased from VWR Collection (Radnor, PA, U.S.). [^{3}H]digoxin (specific activity 39.8, 26.2 or 26.3 Ci·mmol^{-1}), [^{14}C] glycine (99.6 mCi·mmol^{-1}), [^{14}C]mannitol (56.4 mCi·mmol^{-1}), and Ultima Gold were from Perkin Elmer (Waltham, MA, U.S.). Ultrapure water was tapped from a Milli-Q Gradient water purification system from Millipore (Burlington, MA, U.S.).

2.2. Cell cultures

Caco-2 and MDCKII-MDR1 cells were cultivated in Dulbecco's Modified Eagle's Medium supplemented with penicillin (100 units · mL^{-1}), streptomycin (0.1 mg · mL^{-1}), L-glutamine (2 mM), non-essential amino acids (1x) and Foetal Bovine Serum (10%). The cells were incubated at 37 °C and 5% CO_2 in a humidity of approx. 94–97%. The cells were trypsinized once a week at approximately 80% confluency by removing media from the culture flask and rinsing with phosphate-buffered saline. Trypsin-EDTA (3x) was then added, and the cells were incubated for 5–10 mins until detached. Caco-2 cells were seeded on polycarbonate membranes (1.12 cm^2, 0.4 μm pore size) at a density of $8.9{\cdot}10^4$ cells · cm^{-2} and medium was changed every 2–3 days. Bidirectional transport studies were performed using Caco-2 cell monolayer 12–14 days after seeding. The MDCKII-MDR1 cells were seeded in black 96-well plates, clear flat bottom wells (0.33 cm^2), at a density of $2.0{\cdot}10^5$ cells·cm^{-2} and used three days (72 h) after seeding.

2.3. Composition of buffers used for cell studies

Cell experiments unrelated to digestion were performed in Hank's balanced saline solution (HBSS) buffered with 10 mM HEPES and adjusted with NaOH/HCl to pH 7.40 ± 0.01, referred to as 10 mM HEPES (pH 7.4). Digestion was performed in a digestion medium composed of 1.4 mM $CaCl_2$ and 2.0 mM tris maleate adjusted to pH 6.50 ± 0.01 with NaOH/HCl, referred to as digestion medium (pH 6.5). In cell experiments, where digested surfactants were investigated, a separate buffer was used. This buffer was composed of 1 part HBSS, 10x, and 9 parts of the digestion medium (pH 6.5) and was supplemented with 10 mM HEPES. The buffer was adjusted to pH 7.40 ± 0.01 with NaOH/HCl. This buffer was referred to as digestion buffer (pH 7.4). Digestion buffer (pH 7.4) was used when investigating metabolite products and digestion related controls. In assays, where both undigested and digested species were investigated, buffer (pH 7.4) refers to either 10 mM HEPES (pH 7.4) or digestion buffer (pH 7.4). The use of each buffer is specified in the captions in the results section. In P-gp inhibition and cytotoxicity assays in MDCKII-MDR1 cells, calcein-AM was dissolved in DMSO, and the solution was diluted in buffer (pH 7.4) to achieve a final concentration of 10 μM calcein-AM and 1% (v/v) DMSO. The CellTiter-Glo® reagent solution was prepared by adding 0.5 mL buffer (pH 7.4) to 2.5 mL dissolved CellTiter-Glo® Substrate in CellTiter-Glo® Buffer.

2.4. P-gp inhibition- and cell toxicity assay

P-gp inhibition and cell toxicity were assessed in the MDCKII-MDR1 cell line. Inhibition was evaluated using a calcein-AM assay, and cell toxicity was evaluated using the CellTiter-Glo® Luminescent Cell Viability Assay. Surfactant solutions were made in separate 96-well plates through serial dilution. The experiment was initiated by removing the cell culture medium from the wells using vacuum suction (Integra, Zizers, Switzerland). 50 μL of buffer (pH 7.4) was added, and the cells were incubated for 10 min on a microplate shaker (Troemner, Thorofare, NJ, U.S.) at 220 rpm at 37 °C. After this, the buffer was removed, and 50 μL of both surfactant and the 10 μM calcein-AM solution were added to the cells, resulting in a concentration of 5 μM calcein-AM and 0.5% (v/v) DMSO. Fluorescence was read every minute for one

hour at 37 °C using a plate reader with LVF monochromator (CLARIOstar, BMG Labtech, Ortenberg, Germany). Excitation was measured at 483 nm with bandwidth of 14 nm and emission was measured at 530 nm with a bandwidth of 30 nm. After one hour, all solutions were removed and 30 μL of CellTiter-reagent and 50 μL of buffer (pH 7.4) were added to all wells (both at room temperature). In the plate reader, the plate was stirred for two minutes, and luminescence was read every five minutes for a total of 15 min.

2.5. Bidirectional transport of digoxin

Digoxin was used as a marker for P-gp mediated transport, while glycine and mannitol were used as markers for paracellular transport. The activity of [^{3}H]digoxin and [^{14}C]mannitol or [^{14}C]glycine were 1 μCi·mL^{-1} and 0.25 μCi·mL^{-1}, respectively. Stock solutions of [^{3}H] digoxin and the [^{14}C] labeled paracellular markers were prepared, and donor solutions were made by a direct dilution of these stock solutions into buffer (pH 7.4). 96% (v/v) ethanol and buffer (pH 7.4) were used for the [^{3}H]digoxin and [^{14}C] labeled paracellular marker stock solutions, respectively. Digoxin transport was measured in the presence of PS20 (0.2, 2, 20, 200 and 500 μM), Brij-L23 (1, 10, 50, 75 and 100 μM) and Kolliphor EL (15, 30, 100, 250 and 1000 μM). In both absorptive and secretory transport studies, surfactants were only added to the apical chamber. The transport of digoxin in the presence of PS20 ranging from 0.2 μM to 500 μM was performed to validate previous results from Nielsen et al. (2016). Moreover, transport of digoxin in the presence of 500 μM pre-digested PS20 or 75 μM pre-digested Brij-L23 were measured.

Transport of digoxin and paracellular marker was measured in both the absorptive (A-B) and secretory (B-A) direction. 500 μL and 1000 μL were used in the apical and basolateral chamber, respectively. The experiment was initiated by removing the cell culture medium from the wells using vacuum suction. The Caco-2 cells were incubated with buffer (pH 7.4) for 10 min at 220 rpm and 37 °C on a microplate shaker. After incubation, the buffer was removed using vacuum suction. The receiver and donor solutions were added, first to the apical followed by the basolateral chamber. Surfactants diluted in buffer (pH 7.4), both undigested and pre-digested, were only added to the apical chamber to mimic physiological conditions. The receiver sample volume was 100 μL and 50 μL of the basolateral and apical chamber, respectively. Immediately after sampling, equal volumes were replaced with non-radioactive solutions of the same composition. Samples were withdrawn at 20, 40, 60, 90 and 120 min. Donor samples of 20 μL were withdrawn prior to start of the transport experiment and at the end at 120 min. TEER was measured at room temperature before the transport study and after the last sampling at 120 min using an EndOhm-12 chamber (World Precision Instruments, Sarasota, FL, U.S.). After measuring TEER, the filters were rinsed three times with cold HBSS, 1x. Then, all samples were transferred to pony vials, and filters were cut loose and transferred to pony vials. All vials were added 2 mL Ultima Gold scintillation liquid. The samples were vortexed before being analyzed using a liquid scintillation counter (LSC), TriCarb 4910TR from Perkin Elmer (Waltham, MA, U.S.).

2.6. In vitro lipolysis of surfactants

The lipolysis was performed using a titrator instrument composed of a Titrando 905 coupled with an 800 Dosino from Metrohm (Herisau, Switzerland). The chamber was kept at a constant temperature of 37 °C using a thermal jacket. For each lipolysis, 5.5 mL of digestion media (pH 6.5) was added to 1 g of porcine pancreatin and centrifuged for 15 min (4 °C, 4000 rpm, 2800 *g*). Then, 36 mL of digestion media and 1 g of surfactant were added to the chamber and adjusted to pH 6.5 at 37 °C. After initiating the digestion, 4 mL of pancreatin extract supernatant was added to the chamber. Lipolysis continued for 30 min with the pH kept constant at pH 6.5 by adding 0.6 M NaOH. After 30 min, pH was increased to 9.0 using 0.6 M or 1.0 M NaOH to titrate the undigested fraction and thereby to account for the total lipid composition. A sample was transferred from the chamber to a centrifuge tube and placed in a hot water bath to denaturate the lipase proteins in the media. The sample was heated at 60 °C for 5 min. The sample was centrifuged for 15 min (4 °C, 4000 rpm, 2800 *g*) and further dilutions were made with the supernatant. A heat treated, undigested PS20 sample was made to elucidate possible effects of heating and centrifugation on PS20. This control was heated and centrifuged together with the digestion metabolite sample. A blank titration without the addition of surfactant was performed to quantify the degree of digestion. For the digoxin transport assay across Caco-2 cell monolayers, all three digestion degrees of Brij-L23 were averaged for a mean digestion degree and deviation. For PS20, the mean was based on two out of three digestions, as the third digestion degree was beyond 100%. However, as the transport results did not deviate notably, these results were pooled across all three cell passages.

If 4-bromophenylboronic acid (4-BPBA) was used for chemical inhibition instead of heat induced inactivation, a sample from the digestion chamber was drawn before pH was increased to pH 9.0. The sample was added to digestion buffer (pH 7.4) to the desired concentration. 10 μL · mL^{-1} (eq. to 10 mM) of 1 M 4-BPBA in methanol was added to the solution instead of 5 μL · mL^{-1}, as the concentration was halved during the P-gp inhibition assay. This was done to ensure a concentration of 5 μL · mL^{-1} 1 M 4-BPBA during the cell experiments.

2.7. Data analysis

2.7.1. P-gp inhibition

The fluorescence intensity from calcein was plotted as a function of time (min). From this the steady state slope, m, was manually determined for all wells. The remaining P-gp activity at different concentration of added compound was determined as the ratio of slope between exposed cells and the average of the control cells.

$$Remaining\ activity = \frac{m_{control}}{m_{compound}} \times 100\% \quad (1)$$

The P-gp activity or digoxin permeability as a function of the surfactant concentration was fitted to a symmetrical sigmoidal curve in GraphPad v.10.1.0

$$Y = Bottom + \frac{Top - Bottom}{1 + 10^{X - logIC_{50}}} \quad (2)$$

2.7.2. Cell viability

For the cell viability, luminescence in relative light units (RLU) measured in the treated cells were related to control cells. The viability was 100% for control cells, and hence the cell death was estimated using:

$$Cell\ death = 100\% - \left(\frac{RLU_{compound}}{RLU_{control}} \times 100\%\right) \quad (3)$$

2.7.3. Permeability

The apparent permeability was calculated from steady state fluxes using a deviation of Ficks law:

$$J = P_{app} \times C_0 \quad (4)$$

J is the flux from donor to receiver chamber (nmoles · cm^{-2} · min^{-1}), C_0 is the initial donor concentration (nmoles · L^{-1}) and P_{app} is the apparent permeability. An additional calculation was performed to convert P_{app} from cm · min^{-1} to cm · s^{-1}, which is the implemented unit of this paper.

The efflux ratio was calculated using the secretory (B-A) and absorptive (A-B) permeability:

$$Efflux\ ratio = \frac{P_{app\ B-A}}{P_{app\ A-B}} \quad (5)$$

The recovery of isotope during the transport study was calculated as the ratio between the amount of isotope at the end relative to the staring amount:

$$Recovery = \frac{n_{analyte\ end}}{n_{analyte\ initial}} \times 100\% \quad (6)$$

The measured TEER of each insert was adjusted with the area of the filter (1.12 cm^2):

$$TEER_{corrected} = TEER_{measured} \times Filter\ area = \Omega \times cm^2 \quad (7)$$

2.7.4. In vitro digestion

The amount of FFAs released was calculated as the total amount of used NaOH:

$$n_{FFA} = n_{NaOH} = \sum C_{NaOH} \times V_{NaOH} \quad (8)$$

The degree of digestion was determined by the amount of released FFAs:

$$Digestion\% = \frac{n_{FFA}}{n_{surfactant} \times \sum ester\ bonds} \quad (9)$$

2.7.5. Statistics

When possible, results are shown as a mean value ± standard error of the mean (SEM), which was derived from the standard deviation. If multiple technical replicas were performed on the same cell passage, the mean of these replicas (N) were used. When means of more than two groups were compared for significant difference, a one-way ANOVA was used to determine significance within the variables. The ANOVA test was followed by Tukey's multiple comparison test. This was performed in GraphPad Prism. When means of two groups were compared, an F-test for variance and a Student's *t*-test was used. This was done in Excel. $P < 0.05$ was considered significantly different when comparing means. Possible outliers (with a 95% confidence) were excluded using an in-built mechanism of GraphPad v.10.1.0. A single value of remaining P-gp activity when treated with PS20 was determined an outlier and was excluded. The outlier was at 0.65 μM PS20, where 10 technical replicas across three individual cell passages were performed. "n" indicates the amount of individual cell passages.

3. Results

3.1. Undigested surfactants

3.1.1. P-gp inhibition and cell toxicity studies

The concentration-dependent ability of PS20, Brij-L23, Labrasol and Kolliphor EL to inhibit P-gp-mediated transport was investigated using MDCKII-MDR1 cells. Furthermore, the cell viability in the presence of the surfactant was assessed using the CellTiter-Glo® Cell Viability Assay. Increasing the PS20 concentrations showed a concentration-dependent decrease in P-gp activity, as shown in Fig. 1.

The IC_{50} of PS20 was determined to be 10.3 μM ($logIC_{50} = 1.01 \pm 0.09$). The lowest remaining P-gp activity was observed at 500 μM PS20 being 27.1%, however, at this concentration a cell death of 53.8% was observed, whereas at all other concentrations no cell death was observed (Fig. 1A). Similarly, Brij-L23 showed P-gp inhibition, with a maximal decrease in activity of 22.3% at 150 μM, while the lowest concentration of 1.2 μM resulted in an activity of 81.2%. The IC_{50} of Brij-L23 was determined to 32.0 μM ($logIC_{50} = 1.51 \pm 0.20$). Brij-L23 showed toxic effects at both 150 and 75 μM resulting in a death percentage of 79% and 31%, respectively. For Labrasol, P-gp inhibiting effects were observed between 2.8 μM (log = 0.45) and 79 μM (log = 1.9), as depicted in Fig. 1C. However, as evident from all data points, no concentration dependent trend was not present across the investigated concentration range from 2.8 μM to 6.65 mM. When treated with Kolliphor EL, a very small amount of calcein was formed intracellularly, resulting in the P-gp activity reaching beyond 100% as shown in Fig. 1D. This trend was concentration dependent, and already at approximately 1 mM Kolliphor EL (log = 3.01), the determined activity was 3.8 times higher than that of the untreated cells, corresponding to a P-gp activity of 380%. While the results of the inhibition assay were scarce, the viability assay showed a high tolerance towards Kolliphor EL, even at concentrations in the mM range. The MDCKII-MDR1 cells showed better tolerability towards Labrasol than PS20 or Brij-L23, as no toxicity was observed at 724 μM or below.

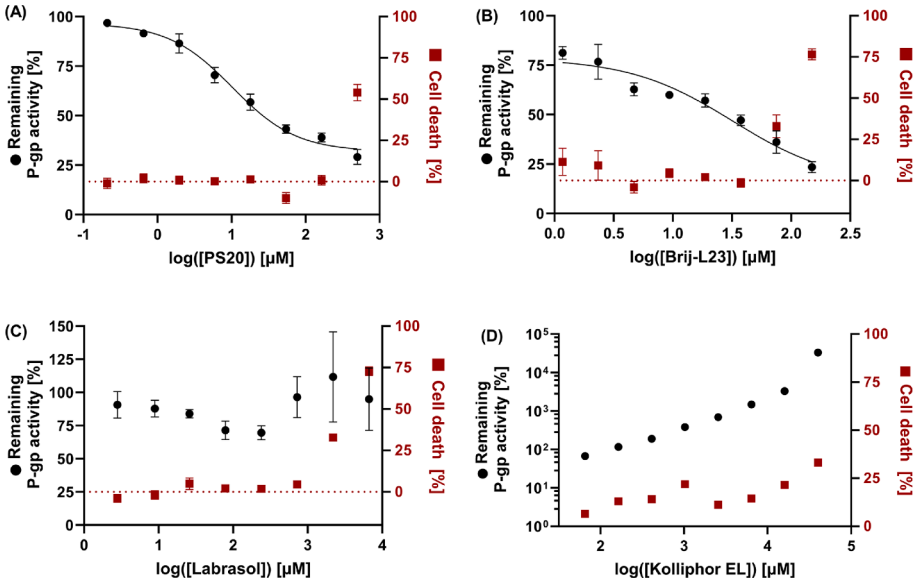

Fig. 1. P-gp inhibition and cell toxicity assay. Cells were treated with solutions of PS20 (A), Brij-L23 (B), Labrasol (C) or Kolliphor EL (D). P-gp inhibition assay was performed at 37 °C for one hour, and the toxicity assay represents one hour exposure to the compounds. A final concentration of 5 μM calcein-AM and 0.5% (v/v) DMSO in 10 mM HEPES (pH 7.4) was used. During the toxicity assay, the luminescence was measured at room temperature for 15 min. Data points of PS20 and Brij-L23 were fitted to a symmetrical sigmoidal curve (equation (2)). Circles (●) represent the remaining P-gp activity, while squares (■) represent the degree of cell death. Each data point represents a mean value ± SEM (n = 3), except for Kolliphor EL, which is a single value. Regarding Labrasol, selected data points of the P-gp activity is shown where cells were viable.

To elucidate the possible effects of surfactant metabolites, likely to originate from digestion, on P-gp inhibition and cell toxicity, the four most common fatty acids (lauric acid, myristic acid, palmitic acid, and stearic acid) were analyzed separately. As seen in Fig. 2, none of the fatty acids showed a concentration-dependent ability to inhibit P-gp activity in MDCKII-MDR1 cells in the concentration range investigated. After exposure to the fatty acid cells generally remained viable.

3.1.2. Digoxin transport across Caco-2 cell monolayers

The concentration-dependent effects of the non-ionic surfactants on digoxin's bidirectional permeability were examined through transport across Caco-2 cell monolayers. In the absence of a surfactant, the transport of digoxin was polarized in the B-A direction, with an efflux ratio (ER) of 11.9 ± 0.5. PS20 was examined in a single determination across the same concentrations as that of Nielsen et al. (2016) to verify that the present data were similar to the published ones. Since the data was comparable and obtained within the same laboratory, the experiment was replicated once to save resources. The studied PS20 concentration ranged from 0.2 to 500 μM and showed an increased absorptive permeability and decreased secretory permeability with an ER approaching 1 at 20 μM. From the bidirectional transport studies, an EC_{50} of PS20 was determined to be 4.4 μM and 4.1 μM in the absorptive and secretory direction, respectively (Fig. 3). No notable drop in final TEER was observed at any PS20 concentration. The highest absorptive P_{app} was $7.1 \cdot 10^{-6}$ cm · s^{-1} at 500 μM, while the lowest secretory P_{app} was $8.2 \cdot 10^{-6}$ cm · s^{-1} at 200 μM, which was the highest concentration of PS20 measured in the secretory direction.

Like PS20, Brij-L23 showed a pronounced increase in the absorptive permeability while decreasing the secretory permeability of digoxin. The ER of digoxin was lowered significantly at 10 μM compared to the control ($P < 0.05$) and approached 1 at 50 μM. An increasing secretory permeability was observed at higher concentrations, starting at 75 μM, while the absorptive permeability continuously increased. The ER remained rather constant at 1.4 ± 0.36 and 1.3 ± 0.23 when treated with 50 μM or 100 μM Brij-L23. The permeability of glycine in each direction did not change notably from 1 to 50 μM, however, the permeability of glycine B-A was significantly larger, compared to the A-B permeability, in both the absence and up to 50 μM of Brij-L23 ($P < 0.05$). This is shown in the supplementary data, Table S 1. At 75 and 100 μM Brij-L23, a time-dependent increase in paracellular transport was observed, depicted in Figure S 1. The time-dependent flux increase was more pronounced in the secretory transport compared to the absorptive transport. In the case of mannitol, no significant difference in permeabilities was observed between A-B and B-A in the absence of Brij-L23 ($P > 0.05$). While no significant decrease in TEER was observed in controls wells ($P > 0.05$), a significant decrease in TEER ($P < 0.05$) was observed at 75 μM and 100 μM Brij-L23, as detailed in Table S 1. Like PS20 and Brij-L23, Kolliphor EL showed a concentration dependent increase in digoxin's absorptive permeability. At a concentration of 1 mM, an ER of 1.3 ± 0.12 was observed. An EC_{50} of 28.8 μM ($\log EC_{50} = 1.46 \pm 0.09$) and 23.9 μM ($\log EC_{50} = 1.38 \pm 0.18$) was determined in the absorptive and secretory direction, respectively. Unlike Brij-L23, no notable change in TEER was observed at any concentration. No correlation between the Kolliphor EL concentration and paracellular transport of mannitol was observed, and the permeabilities of mannitol were comparable to that of the control. All efflux ratios are presented in Table S 1 and the recovery of digoxin, glycine and mannitol is presented in Table S 2.

3.2. Assessment of the impact of standardized in vitro digestion on cell-based assays

The digestion medium used by Koehl and coworkers included 150 mM NaCl (Koehl et al., (2020)). As the final digestion buffer would be highly hyperosmotic, which would impair cell barrier integrity, the importance of NaCl was examined. A degree of digestion of 41.7% was observed for PS20 with 150 mM NaCl, while 42.0% digestion was observed without NaCl. Hence, NaCl was excluded from the digestion medium for further studies. The study by Koehl et al. (2020) used 5 mM 4-BPBA to inactivate the lipases from the pancreatin. As 4-BPBA would be part of the pre-digested solution applied to cells, a P-gp inhibition and cell toxicity assay examining the effects of 4-BPBA in digestion buffer (pH 7.4) was performed. The assays showed a concentration dependent cell toxicity of 4-BPBA, which did not differ notably after the precipitate was discarded by centrifugation (Fig. 4). The dotted line in A and B indicates the suggested concentration of 4-BPBA of 5 μL · mL^{-1} (corresponding to 5 mM). At this concentration, a consistent effect on the formation of calcein as well as persistent cytotoxicity was observed. It was evident, that 4-BPBA affected both the calcein-AM assay and the cell viability assay. Due to the observed toxicity, inactivation of lipase activity was instead performed by heat denaturation.

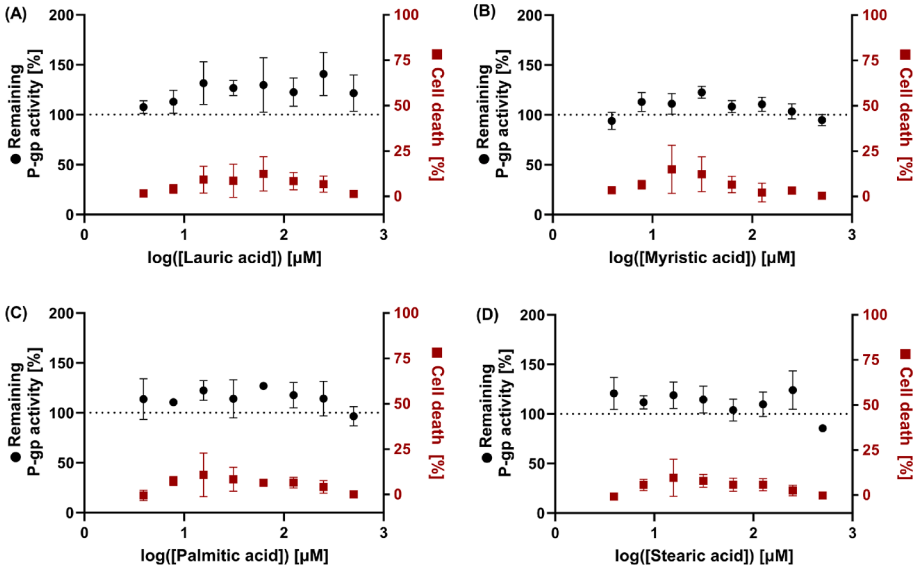

Fig. 2. P-gp inhibition and cell toxicity assay. Cells were treated with solutions of lauric acid (A), myristic acid (B), palmitic acid (C) or stearic acid (D). P-gp inhibition assay was performed at 37 °C for one hour, and the toxicity assay represents one hour exposure to the compounds. A final concentration of 5 μM calcein-AM and 0.5% (v/v) DMSO in 10 mM HEPES (pH 7.4) was used. During the toxicity assay, the luminescence was measured at room temperature for 15 min. Circles (●) represent the remaining P-gp activity, while squares (■) represent the degree of cell death. Each data point represents a mean value ± SEM (n = 3).

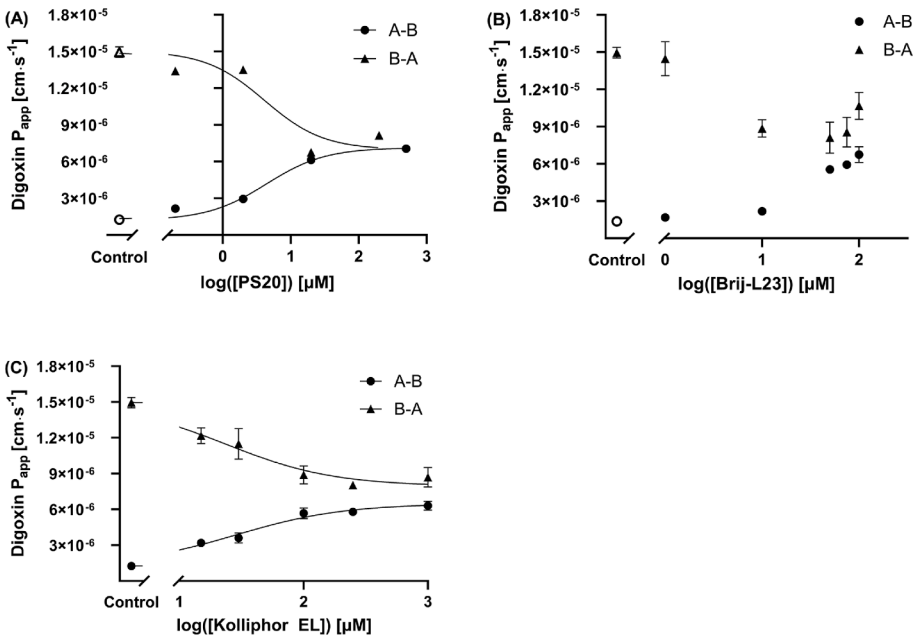

Fig. 3. Bidirectional permeability studies of digoxin across a Caco-2 cell monolayer in the presence of PS20 (A) at concentrations of 0.2, 2.0, 20, 200 and 500 μM, Brij-L23 (B) at concentrations of 1, 10, 50, 75 and 100 μM or Kolliphor EL (C) at concentrations of 15, 30, 100, 250 and 1000 μM. Surfactants dissolved in 10 mM HEPES (pH 7.4), were only added to the apical chambers while basolateral chambers were filled 10 mM HEPES (pH 7.4). Donor activity was 1 μCi · mL^{-1} for [^{3}H] digoxin and 0.25 μCi · mL^{-1} for [^{14}C]glycine or [^{14}C]mannitol. All wells were pre-incubated with 10 mM HEPES (pH 7.4) for 10 min (220 rpm, 37 °C). PS20 and Kolliphor EL were fitted to symmetrical sigmoidal curve (equation (2)) for each direction. Control studies in the absence of surfactants are shown at the far-left x-axis (n = 8). For PS20 each represents a single point (n = 1). Regarding Brij-L23 and Kolliphor EL, each represents a mean ± SEM (n = 3).

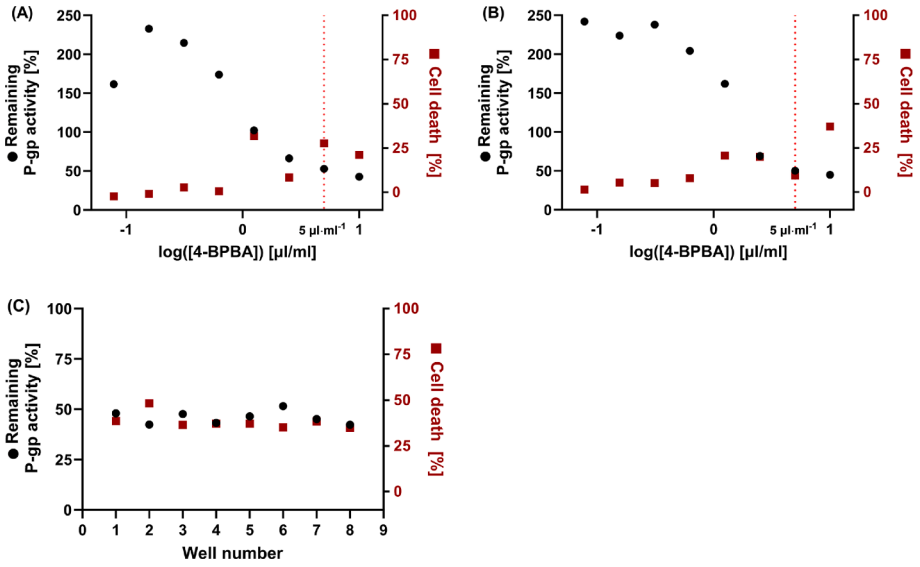

Fig. 4. P-gp inhibition and cell toxicity assay. Cells were treated with dilutions of 1 M 4-BPBA in digestion buffer (pH 7.4) measured in μL · mL^{-1}. In (A), 4-BPBA was dispersed in the digestion buffer (pH 7.4). In (B), 4-BPBA was dispersed in digestion buffer (pH 7.4) followed by 15 min of centrifugation (4 °C, 4000 rpm, 2800 g). The supernatant was isolated and used for the assay. In (C), the effects of a constant concentration of 5 μL · mL^{-1} (5 mM) were examined in 8 wells. P-gp inhibition assay was performed at 37 °C for one hour, and the toxicity assay represents one hour exposure to the compound. A final concentration of 5 μM calcein-AM and 0.5 % (v/v) DMSO in digestion buffer (pH 7.4) was used. During the toxicity assay, the luminescence was measured at room temperature for 15 min. Circles (●) represent the remaining P-gp activity, while squares (■) represent the degree of cell death. Each data point represents single value.

3.3. *Pre-digested surfactants*

Chaitanya and Prabhu (2014) reported that porcine lipases undergo irreversible unfolding and subsequently lose activity when heated to 45 °C, supporting the use of heat to inactivate the enzymes after digestion. Digestion samples were denatured at 60 °C for 5 min together with a PS20 solution used as a heat treated, undigested PS20 control. Samples from the supernatant were diluted in digestion buffer (pH 7.4) to reach the desired concentrations. The stated concentrations were not corrected for the degrees of digestion but were based on the initial surfactant concentration prior to the digestion. All pre-digested species and corresponding control treatments were diluted in digestion buffer (pH 7.4) unless otherwise stated. The digestion buffer (pH 7.4) itself did not affect P-gp in any way and was comparable to that of 10 mM HEPES

(pH 7.4).

3.3.1. P-gp inhibition and cell toxicity of pre-digested surfactants

For the P-gp inhibition assays, the degree of digestion for PS20 was 42 ± 6% and resulted in an IC_{50} of 18.7 μM ($logIC_{50} = 1.27 \pm 0.17$) as depicted in Fig. 5A. The corresponding IC_{50} values of the heated, undigested PS20 and the undigested PS20 was 15.3 μM ($logIC_{50} = 1.18 \pm 0.21$) and 26.9 μM ($logIC_{50} = 1.43 \pm 0.20$), respectively. Therefore, the obtained IC_{50} values did not differ significantly between the undigested and digested PS20 species. However, the observed cytotoxicity was lower in the pre-digested samples as compared to the undigested species, both in digestion buffer (pH 7.4) and 10 mM HEPES (pH 7.4), reflecting a correlation between the cell toxicity and amount of intact PS20. In the pre-digested samples, the highest PS20 concentration of 500 μM resulted in 14% cell death, whereas the undigested and the heated, undigested PS20 reached 47% and 46% at the same concentration, respectively. However, the reduction observed in the pre-digested species was not significantly lower than any of the undigested species ($P > 0.05$).

As the IC_{50} values of the pre-digested and undigested PS20 samples did not differ notably from one another across the full concentration range, the two most critical PS20 concentrations were chosen for further comparison. All curves showed a dynamic area around 18 μM and 6 μM PS20, where the change in P-gp activity was at its highest, i.e. the middle section of the curves with the steepest slope. To elucidate the differences between the pre-digested and undigested PS20, the remaining P-gp activities at these concentrations were compared between all PS20 species from this investigation, as depicted in Fig. 6.

The results showed that no significant difference ($P > 0.05$) was present between solutions. A difference between buffers was observed when treated with 6 μM PS20, where the activity of 10 mM HEPES (pH 7.4) treated cells were slightly lower compared to that of the digestion buffer (pH 7.4) treated cells. At 18 μM PS20 the means of each group were more aligned with smaller deviations. The differences in P-gp activities were not significant ($P > 0.05$) between the examined species; pre-digested or undigested.

3.3.2. Digoxin transport across Caco-2 cell monolayers

Brij-L23 and PS20 were pre-digested *in vitro,* and the products were diluted to 75 μM and 500 μM, respectively. The digestion degree of Brij-L23 was negligible and PS20 had a mean degree of digestion of 46%. In the presence of pre-digested surfactants, digoxin showed P_{app} values, both absorptive and secretory, close to those of the undigested surfactants (Fig. 7). This was further shown by the efflux ratio, which is displayed above the grouped columns in Fig. 7.

75 μM pre-digested Brij-L23, as opposed to 500 μM PS20, affected the resulting TEER notably. The final TEER in the absorptive and secretory direction was 120 $\Omega \cdot cm^2$ and 45 $\Omega \cdot cm^2$, respectively, when treated with 75 μM pre-digested Brij-L23. This was notably lower than that of the digestion buffer (pH 7.4) control, which was 386 $\Omega \cdot cm^2$ in the absorptive direction, and 360 $\Omega \cdot cm^2$secretory direction, at the end of the experiment, as shown in Table S 3. A significant increase ($P < 0.05$) in secretory mannitol flux at 120 min was observed between 75 μM pre-digested Brij-L23 and the digestion buffer (pH 7.4) control, depicted in Figure S 2. As TEER was not measured for all cell passages, the significance could not be determined. The recovery of digoxin and mannitol is presented in Table S 4.

4. Discussion

The present study investigated if surfactants exposed to *in vitro* intestinal digestion are likely to maintain their P-gp inhibiting properties, or if digestion is likely to explain the large *in vitro* to *in vivo* discrepancy observed for the dose/concentration of surfactants required to increase the absorption of P-gp substrates. The P-gp inhibiting abilities of the non-ionic surfactants were investigated through bidirectional digoxin transport across Caco-2 cell monolayers and specifically for their P-gp inhibitory properties using the calcein-AM efflux in MDCKII-MDR1 cells assay.

4.1. The traditional digestion setup is incompatible with cell assays

4-BPBA is a commonly used inactivator of pancreatic lipases, as it potently inactivates the enzymes at 5 mM (Mulet-Cabero et al., (2020)).

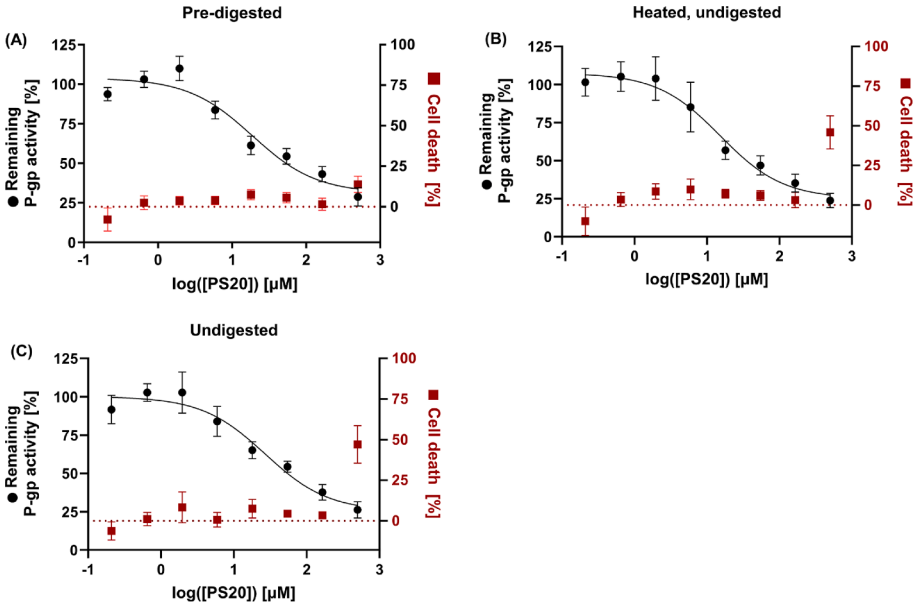

Fig. 5. P-gp inhibition and cell toxicity assay. Cells were treated with solutions of pre-digested PS20 (A), heated, undigested PS20 (B) or undigested PS20 (C), all diluted in digestion buffer (pH 7.4). The heated, undigested PS20 sample underwent same heating and centrifugation procedure as the pre-digested sample. P-gp inhibition assay was performed at 37 °C for one hour, and the toxicity assay represents one hour exposure to the compound. A final concentration of 5 μM calcein-AM and 0.5% (v/v) DMSO in digestion buffer (pH 7.4) was used. During the toxicity assay, the luminescence was measured at room temperature for 10 min. Data points were fitted to a symmetrical sigmoidal curve (equation (2). Circles (●) represent the remaining P-gp activity, while squares (■) represent the degree of cell death. Each data point represents a mean value ± SEM (n = 4).

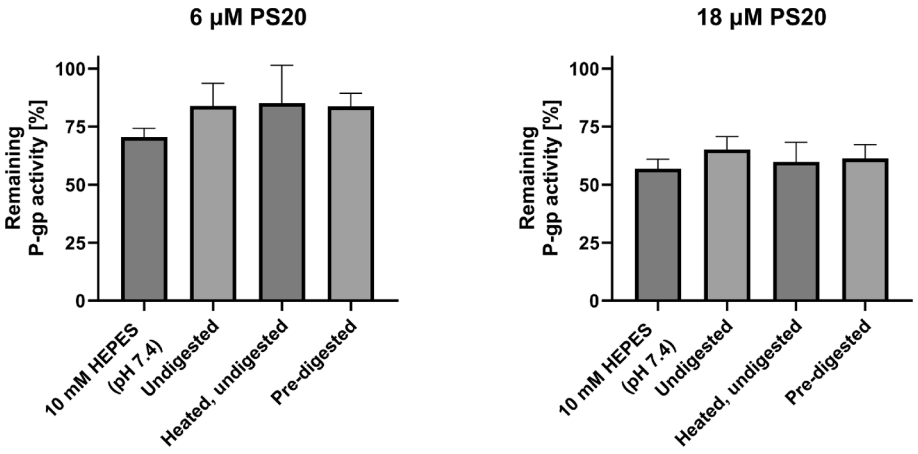

Fig. 6. Elucidation of the effect of pre-digestion on PS20's ability to inhibit the P-gp transporter in MDCKII-MDR1 cells. Activities of all controls and buffers were compared across two different concentrations of PS20. Cells were treated with solutions of undigested or pre-digested PS20 in either 10 mM HEPES (pH 7.4) or digestion buffer (pH 7.4). P-gp inhibition assay was performed at 37 °C and fluorescence was measured for one hour. A final concentration of 5 µM calcein-AM and 0.5% (v/v) DMSO in buffer (pH 7.4) was used. Each data set represents a mean ± SEM (n = 3–4).

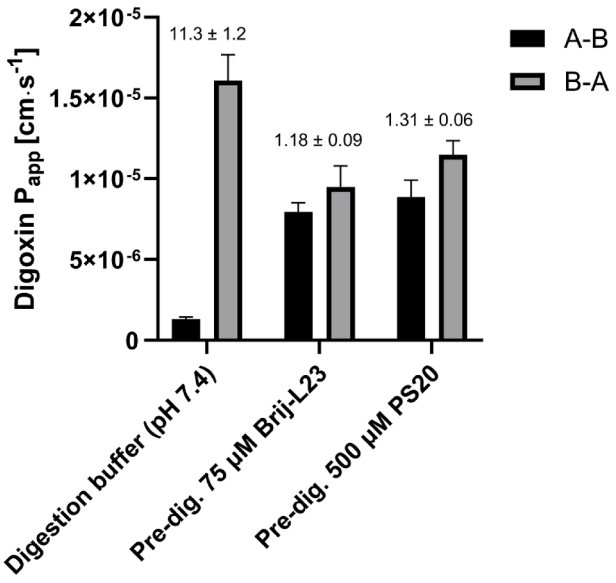

Fig. 7. Bidirectional permeability studies of digoxin across a Caco-2 cell monolayer in the presence of pre-digested Brij-L23 (75 µM) or PS20 (500 µM). Surfactants dissolved in Digestion buffer (pH 7.4), were only added to the apical chambers while basolateral chambers were filled with digestion buffer (pH 7.4). Donor activity was 1 µCi · mL^{-1} for [^{3}H]digoxin and 0.25 µCi · mL^{-1} for [^{14}C] glycine or [^{14}C]mannitol. All wells were pre-incubated with digestion buffer (pH 7.4) for 10 min (220 rpm, 37 ∘C). Figure shows the absorptive and secretory permeabilities of surfactants or controls. Each value represents a mean ± SEM (n = 3). The number beyond each group is the mean efflux ratio of said group.

However, as evident from the assays in the MDCKII-MDR1 cell line, 4-BPBA affects both the formation of calcein and shows notable cytotoxic effects. While a reduced concentration of 2.5 mM has been used in some studies, the cytotoxic effects were observed below this concentration. Because more biomimetic setups for dissolution and permeation is desired, the cytotoxicity of the typical lipase inhibitor composed a problem. Here we solved this by using heat mediated denaturation at 60 °C to inactivate the lipases without any observed effects on neither calcein formation nor cell cytotoxicity. This method was based on the findings of Chaitanya and Prabhu (2014), who reported that porcine lipase underwent irreversible unfolding and lost its activity when heated to 45 °C. The cell disrupting effects of the pancreatic enzymes has been reported by Keemink and Bergström (2018), who observed an incompatibility between Caco-2 cells and pancreatic extract at the concentration used in a standardized *in vitro* lipolysis. While the presence of neither low nor high concentrations of mucin increased compatibility notably, Keemink and Bergström showed, that immobilized lipase was compatible with Caco-2 cells, even in the absence of mucin. Furthermore, the study introduced digestion samples of lipid-based formulations in a digestion buffer composed of Tris–maleate, $CaCl_2$, NaCl, sodium taurocholate and lecithin. In the absence of mucin, the mixture with an initial 2.5% (w/v) lipid formulation did disrupt the Caco-2 cell layer integrity. However, in the presence of mucin the formulations were compatible. In contrast to the present study, the digestion samples used by Keemink and Bergström did include 5 µL · mL^{-1} 0.5 M 4-BPBA without observing any reported adverse effects. Despite this, 4-BPBA was excluded from the present study based on the observed toxicity and incompatibility with the MDCKII-MDR1 cell assays. According to the results obtained by Keemink and Bergström, the digestion media with 150 mM NaCl adjusted to pH 7.40 would likely be a compatible buffer with the Caco-2 cells during the transport of digoxin in the present study. However, the presence of both 150 mM NaCl from the digestion media and HBSS, 1x, resulted in a hyperosmotic buffer. To conserve the conditions present in the studies of the undigested surfactants, the digestion buffer composed of HBSS, 1x, and 10 mM HEPES was favored, and 150 mM NaCl was subsequently excluded from the digestion media. This decision was supported by the data showing, that digestion of PS20 was independent of NaCl.

4.2. Labrasol shows no clear concentration dependent P-gp inhibition

Whilst the determined P-gp activities in the MDCKII-MDR1 cell line in the presence of 2.8 to 78.9 µM Labrasol did indicate a concentration dependent P-gp inhibition, the activities across the entire concentration range from 2.8 µM to 6.6 mM revealed, that there was no clear concentration dependent effect on P-gp inhibition. There seems to be two potential explanations for this, one being the formation of micelles and the other cellular toxicity at higher concentrations. At concentrations above 78.9 µM, the critical micelle concentration of Labrasol (approximately 140 µM (GatteFossé (2023)) is exceeded and micelles are formed. This may entrap calcein-AM in the micelles, and hence reduce the free concentration, and shade the actual P-gp inhibition due to a reduced cellular uptake of the calcein-AM. Labrasol has previously been reported to increase the absorptive transport and decrease the secretory transport of rhodamine123 across rat ileum *in vitro* at 0.075% (v/v) (Lin et al., (2007)). While the study by Lin and coworkers observed a 66% decrease

in the efflux ratio, the polarized transport in the absence of Labrasol corresponded to an ER of 2.67, compared to that of digoxin in this study being 11.9. Furthermore, Lin and coworkers observed a significant increase in the absorptive permeability of the paracellular marker lucifer yellow in the ileum in the presence of 0.1% (v/v) Labrasol. From these findings, Lin et al. concluded that the increased transport of Rhodamine123 was likely not caused by P-gp inhibition solely, but also caused by an increased paracellular transport. In contrast to Labrasol, the P-gp inhibiting abilities of Kolliphor EL has been reported during transport of P-gp substrates across Caco-2 cell monolayers, why Labrasol was substituted with Kolliphor EL for transport assays (Rege et al., (2002)). The P-gp inhibition properties of Kolliphor EL was therefore investigated in MDCKII-MDR1 cells using the calcein-AM assay. However, testing Kolliphor EL in this assay was not experimentally possible since very low fluorescence was recorded.

4.3. P-gp inhibition is not affected by pancreatin mediated intestinal digestion

PS20 has in numerous studies been shown to increase the *in vitro* absorption of P-gp substrates (Al-Ali et al., (2018a); Nielsen et al. (2016); Al-Saraf et al. (2016)). The present study found values for the undigested PS20 in accordance with the data reported by Nielsen et al. (2016), with respect to both the absorptive and secretory permeabilities of digoxin. Nielsen and coworkers reported an absorptive EC_{50} of 25.0 μM and secretory EC_{50} of 4.9 μM. Compared to the absorptive and secretory EC_{50} values of this study, where the corresponding EC_{50} values were 4.4 and 4.1 μM, respectively, the P-gp inhibiting ability of PS20 was evident. Furthermore, similar to the present study, Nielsen and coworkers observed no notable drop in the finale TEER of cells treated with PS20 compared to that, of cells treated purely with 10 mM HEPES (pH 7.4). The P-gp inhibiting ability of PS20 was furtherly investigated in the MDCKII-MDR1 cells, where the determined IC_{50} value towards P-gp was similar to that of Al-Ali et al., (2018b), who determined an IC_{50} value of 11 μM utilizing the same calcein-AM based assay in MDCKII-MDR1 cells. P-gp inhibition mediated by non-ionic surfactants is believed to occur by various mechanisms, including changes in membrane fluidity and direct binding to the P-gp transporter. Li-Blatter and Seelig (2010) suggested, that only the polar moieties of PS20′s ethoxylated chains bind directly to P-gp. Moesgaard et al. (2022) verified the hydrogen bonds emerging between the PEG moieties of PS20 and the drug binding cavity of P-gp using molecular dynamics. Moesgaard and coworkers proposed, that PS20 form a “lollipop” structure in the cell membrane, with PEG aggregating towards the outer membrane leaflet, and the lipid chain extending towards the lipophilic core of the membrane. PS80, a similar non-ionic surfactant with the same lipid chain as PS20, has been reported to notably increase membrane fluidity with the anisotropy decreasing to 50.9%, corresponding to an increased fluidity of the inner membrane core of Caco-2 cells (Rege et al., (2002)). The findings of the present study suggested that the partitioning of intact PS20 into the membrane was not the driving factor of P-gp inhibition, evident by the degree of P-gp inhibition not varying significantly between the undigested and pre-digested species. This was in spite of the observed degree of digestion, which limited the amount of lipid chains present, that was able to partition into the membrane. The suggestion, that only the hydrogen bonds of the PEG domains mediate the P-gp inhibition corresponds with the abilities of pure PEG to inhibit P-gp (Shen et al., (2006)). PEG-400 and PEG-20,000 have both shown to inhibit P-gp, both *in vitro* and *in situ* during Rhodamine123 transport across rat jejunal membrane. With 5% (w/v) PEG-20,000 the efflux ratio was reduced from 7.73 to 2.16 without any significant effect on the transport of lucifer yellow (Shen et al., (2006)). The possible effects of the lipid chains released during PS20 digestion were investigated using the commercially available compounds. The examined concentrations were equal to that of the undigested and pre-digested PS20 to compare the fatty acids’ possible effect on P-gp activity and cell toxicity levels adequately to that of PS20. Furthermore, this concentration range would mimic the contribution of the released fatty acids present in the mixture, in case the degree of digestion was near 100%. Whilst the lipid chain of PS20 did not contribute to P-gp inhibition, it may, however, contribute to the PS20 mediated cytotoxicity observed in the MDCKII-MDR1 cells at 500 μM. The pre-digested species showed notably lower degrees of cell death compared to the undigested counterparts. However, the examination of the typically released fatty acids of PS20 did not result in the same degree of cell death at 500 μM, indicating that the lipid chain is not the only contributor to PS20 mediated cell toxicity.

Brij-L23, a non-ionic surfactant composed of only one PEG moiety and a lipid chain, has previous been shown to increase the absorptive transport of rhodamine123 across washed rat intestines at 0.5% (w/v) Brij-L23 (Iqbal et al., (2010)). Furthermore, bidirectional transport across Caco-2 cell performed by Yu et al. (2011) showed a concentration-dependent decrease in the efflux ratio of the P-gp substrate bis(12)-hupyridone when Brij-L23 was present both apical and basolateral. Similar findings on Brij-L23′s ability to inhibit the efflux transporter was observed in the present study. Furthermore, an effect on barrier properties was established, as the observed increase in paracellular transport of glycine and mannitol across Caco-2 cells treated with 75 μM and 100 μM Brij-L23 was likely linked to cell toxicity. While this study observed a degree of cell death reaching 30% and 79% in the MDCKII-MDR1 cells treated with 75 μM and 150 μM Brij-L23, respectively, the study by Yu and coworkers reported a 40 % cell death at 120 μM in the Caco-2 cells. These concentrations and corresponding degrees of cell death correlates with the observed flux increase of paracellular markers in the present study. This study verified, that Brij-L23 solutions exposed to the digestion enzymes of pancreatin did not alter the transport of digoxin across Caco-2 cell monolayers. Furthermore, this study concluded, that Brij-L23 could affect both the absorptive and secretory transport of a P-gp substrate, whilst only being present in the apical chamber. This suggests, that Brij-L23 possess the ability to inhibit P-gp without crossing the apical membrane of the enterocyte. The mechanism behind the P-gp inhibition mediated by Brij-L23 is unknown, however, based on the composition of Brij-L23, the mechanism is likely similar to that of PS20, where a similar lollipop structure could emerge. The presence of the same lollipop structure could be supported by the findings of Behzadipour et al. (2001), who showed that Brij 58, a similar non-ionic surfactant, partitioned into the lipophilic membrane core of corn cells, resulting in an increased fluidity. However, as described for PS20, only the PEG-domain of Brij-L23 was suspected to interact with P-gp, whereas the lipid chain likely played no crucial role in the inhibition of the efflux transporter.

In agreement with the findings of Rege et al. (2002), Kolliphor EL increased the absorptive permeability and decreased the secretory permeability of digoxin, resulting in an ER below two. In contrast to the transport of digoxin, the inclusion of Kolliphor EL in the P-gp inhibition assay in MDCKII-MDR1 did not result in any useful data. As all but one of the investigated Kolliphor EL concentrations were beyond the critical micelle concentration, which is approximately 80 μM (SigmaAldrich (2023)), it was suspected that calcein-AM partitioned into micelles, resulting in low intracellular accumulation of calcein-AM. However, a study by Hugger et al. (2002) saw the same tendency, where 0.1% (w/v) Kolliphor EL, approximately 400 μM, inhibited P-gp mediated efflux in Caco-2 cell monolayers, but not MDCKII-MDR1 cell monolayers, indicating a dependency of the cell line. The authors suggested that the difference could be caused by the different environment around the efflux transporter in the two cell lines. The same study by Hugger and coworkers showed, that Kollliphor EL was not able to alter membrane fluidity at 400 μM and concluded, that no connection between membrane fluidity and Kolliphor EL mediated P-gp inhibition was found. The ability to alter membrane fluidity was likely concentration dependent, as evident by Rege et al. (2002), who found that 1 mM Kolliphor EL increased the fluidity of the hydrophobic core of the membrane in Caco-2 cells. Whilst both studies observed P-gp inhibition, the results

indicated that the inhibition was not caused solely by increased membrane fluidity. Thus, the presence of the PEG domains in Kolliphor EL was likely to be a large contributor of P-gp inhibition. Kolliphor EL was partially digested by pancreatin, resulting in the hydrolysis of the lipid chains (Koehl et al., (2020)). However, as the surfactant composes three ester bonds, Kolliphor EL may still be able to partition into the cell membrane upon digestion, depending on the remaining number of lipid chains. Furthermore, the PEG moieties were not affected by hydrolysis, and the P-gp inhibiting abilities of the metabolite would likely be similar to that of pre-digested PS20 and Brij-L23; unaltered.

Using an *in vitro* digestion setup, this study has shown that intestinal digestion did not alter the abilities of the non-ionic surfactants to inhibit P-gp. Both the digestible PS20 and undigestible Brij-L23 increased the absorptive transport whilst decreasing the secretory transport of digoxin across Caco-2 cell monolayers in both their undigested and pre-digested form. Furthermore, the pre-digestion of PS20 elucidated, that the P-gp activity in MDCKII-MDR1 cells did not change significantly between the pre-digested and undigested species. The findings suggested that the inhibition of the efflux transporter was mediated mainly by direct interactions between the non-ionic surfactants and the transporter. The observed discrepancy between *in vitro* and *in vivo* on the needed concentration or dose could potentially be explained by surfactant dilution in rats, which lowered the effective concentration for P-gp inhibition.

5. Conclusion

In conclusion, polysorbate 20, Brij-L23 and Kolliphor EL was shown to increase the absorptive transport of digoxin across Caco-2 cell monolayers while decreasing the secretory transport. The individual EC_{50} values of the surfactants effect on the absorptive and secretory transport varied. Polysorbate 20 and Brij-L23 showed a concentration dependent inhibition of P-gp, however, both surfactants introduced cell toxicity at high concentrations. Neither the indigestible Brij-L23 nor the digestible polysorbate 20 resulted in any noteworthy differences in digoxin permeabilities across Caco-2 cell monolayers when compared to their undigested counterparts. The total digestion metabolite mixture of polysorbate 20 had similar P-gp inhibiting effects in MDCKII-MDR1 cells when compared to the undigested surfactants, however, as the individual lipids showed no inhibition this suggested that the PEG-containing moiety could be the functional mediator of the observed inhibition. From the results, the intestinal digestion of non-ionic surfactants is likely not the cause of the discrepancy in dose required to elicit an inhibition of P-gp observed between *in vitro* and *in vivo* studies.

CRediT authorship contribution statement

Asbjørn Jaensch Rasmussen: Writing – review & editing, Writing – original draft, Visualization, Methodology, Formal analysis, Conceptualization. **Maria Pedersen:** Writing – review & editing, Writing – original draft, Methodology, Investigation, Formal analysis, Conceptualization. **Brendan T. Griffin:** Writing – review & editing, Methodology, Conceptualization. **René Holm:** Writing – review & editing, Writing – original draft, Supervision, Resources, Methodology, Conceptualization. **Carsten Uhd Nielsen:** Writing – review & editing, Writing – original draft, Supervision, Resources, Project administration, Methodology, Investigation, Formal analysis, Conceptualization.

Declaration of competing interest

The authors declare that they have no known competing financial interests or personal relationships that could have appeared to influence the work reported in this paper.

Data availability

Data will be made available on request.

Acknowledgements

We would like to thank the Carlsberg Foundation, case number CF20-0270, (Copenhagen, Denmark) for granting the plate reader system used for the P-gp inhibition and cell toxicity assays.

Appendix A. Supplementary material

Supplementary data to this article can be found online at https://doi.org/10.1016/j.ijpharm.2024.124120.

References

Al-Ali, A.A.A., Quach, J.R.C., Bundgaard, C., Steffansen, B., Holm, R., Nielsen, C.U., 2018a. Polysorbate 20 alters the oral bioavailability of etoposide in wild type and mdr1a deficient Sprague-Dawley rats. Int. J. Pharm. 543, 352–360. https://doi.org/10.1016/j.ijpharm.2018.04.006.

Al-Ali, A.A.A., Steffansen, B., Holm, R., Nielsen, C.U., 2018b. Nonionic surfactants increase digoxin absorption in Caco-2 and MDCKII MDR1 cells: Impact on P-glycoprotein inhibition, barrier function, and repeated cellular exposure. Int. J. Pharm. 551, 270–280. https://doi.org/10.1016/j.ijpharm.2018.09.039.

Al-Ali, A.A.A., Nielsen, R.B., Steffansen, B., Holm, R., Nielsen, C.U., 2019. Nonionic surfactants modulate the transport activity of ATP-binding cassette (ABC) transporters and solute carriers (SLC): Relevance to oral drug absorption. Int. J. Pharm. 566, 410–433. https://doi.org/10.1016/j.ijpharm.2019.05.033.

Ali, B., Jamal, Q.M., Mir, S.R., Shams, S., Al-Wabel, N.A., Kamal, M.A., 2015. In silico analysis for predicting fatty acids of black cumin oil as inhibitors of P-glycoprotein. Pharmacogn. Mag. 11, S606–S610. https://doi.org/10.4103/0973-1296.172969.

Al-Saraf, A., Holm, R., Nielsen, C.U., 2016. Tween 20 increases intestinal transport of doxorubicin in vitro but not in vivo. Int. J. Pharm. 498, 66–69. https://doi.org/10.1016/j.ijpharm.2015.12.017.

Aspenström-Fagerlund, B., Tallkvist, J., Ilbäck, N.-G., Glynn, A.W., 2012. Oleic acid decreases BCRP mediated efflux of mitoxantrone in Caco-2 cell monolayers. Food Chem. Toxicol. 50, 3635–3645. https://doi.org/10.1016/j.fct.2012.07.015.

Behzadipour, M., Kluge, M., Lüthje, S., 2001. Changes in plasma membrane fluidity of corn (Zea mays L.) roots after Brij 58 treatment. Protoplasma 217, 65–69. https://doi.org/10.1007/bf01289415.

Chaitanya, P.K., Prabhu, N.P., 2014. Stability and activity of porcine lipase against temperature and chemical denaturants. Appl. Biochem. Biotechnol. 174, 2711–2724. https://doi.org/10.1007/s12010-014-1220-8.

Cornaire, G., Woodley, J., Hermann, P., Cloarec, A., Arellano, C., Houin, G., 2004. Impact of excipients on the absorption of P-glycoprotein substrates in vitro and in vivo. Int. J. Pharm. 278, 119–131. https://doi.org/10.1016/j.ijpharm.2004.03.001.

GatteFossé, 2023. Labrasol®. Accessed 10-12, 2023. https://www.gattefosse.com/pharmaceuticals/product-finder/labrasol.

Gurjar, R., Chan, C., Curley, P., Sharp, J., Chiong, J., Rannard, S., Siccardi, M., Owen, A., 2018. Inhibitory effects of commonly used excipients on P-glycoprotein in vitro. Mol. Pharm. 15, 4835–4842. https://doi.org/10.1021/acs.molpharmaceut.8b00482.

Houshaymi, B., Nasreddine, N., Kedees, M., Soayfane, Z., 2019. Oleic acid increases uptake and decreases the P-gp-mediated efflux of the veterinary anthelmintic Ivermectin. Drug. Res. (Stuttg.) 69, 173–180. https://doi.org/10.1055/a-0662-5741.

Hugger, E.D., Novak, B.L., Burton, P.S., Audus, K.L., Borchardt, R.T., 2002. A comparison of commonly used polyethoxylated pharmaceutical excipients on their ability to inhibit P-glycoprotein activity in vitro. J. Pharm. Sci. 91, 1991–2002. https://doi.org/10.1002/jps.10176.

Iqbal, J., Hombach, J., Matuszczak, B., Bernkop-Schnürch, A., 2010. Design and in vitro evaluation of a novel polymeric P-glycoprotein (P-gp) inhibitor. J. Control. Release 147, 62–69. https://doi.org/10.1016/j.jconrel.2010.06.023.

Keemink, J., Bergström, C.A.S., 2018. Caco-2 cell conditions enabling studies of drug absorption from digestible lipid-based formulations. Pharm. Res. 35, 74. https://doi.org/10.1007/s11095-017-2327-8.

Kitagawa, S., Nabekura, T., Kamiyama, S., Takahashi, T., Nakamura, Y., Kashiwada, Y., Ikeshiro, Y., 2005. Effects of alkyl gallates on P-glycoprotein function. Biochem. Pharmacol. 70, 1262–1266. https://doi.org/10.1016/j.bcp.2005.07.013.

Koehl, N.J., Holm, R., Kuentz, M., Jannin, V., Griffin, B.T., 2020. Exploring the impact of surfactant type and digestion: Highly digestible surfactants improve oral bioavailability of Nilotinib. Mol. Pharm. 17, 3202–3213. https://doi.org/10.1021/acs.molpharmaceut.0c00305.

Leslie, E.M., Deeley, R.G., Cole, S.P., 2005. Multidrug resistance proteins: role of P-glycoprotein, MRP1, MRP2, and BCRP (ABCG2) in tissue defense. Toxicol. Appl. Pharmacol. 204, 216–237. https://doi.org/10.1016/j.taap.2004.10.012.

Li-Blatter, X., Seelig, A., 2010. Exploring the P-glycoprotein binding cavity with polyoxyethylene alkyl ethers. Biophys. J. 99, 3589–3598. https://doi.org/10.1016/j.bpj.2010.10.033.

Lin, Y., Shen, Q., Katsumi, H., Okada, N., Fujita, T., Jiang, X., Yamamoto, A., 2007. Effects of Labrasol and other pharmaceutical excipients on the intestinal transport and absorption of rhodamine123, a P-glycoprotein substrate, in rats. Biol. Pharm. Bull. 30, 1301–1307. https://doi.org/10.1248/bpb.30.1301.

Lin, J.H., Yamazaki, M., 2003. Role of P-glycoprotein in pharmacokinetics: Clinical implications. Clin. Pharmacokinet. 42, 59–98. https://doi.org/10.2165/00003088-200342010-00003.

Lo, Y.L., 2003. Relationships between the hydrophilic-lipophilic balance values of pharmaceutical excipients and their multidrug resistance modulating effect in Caco-2 cells and rat intestines. J. Control. Release 90, 37–48. https://doi.org/10.1016/s0168-3659(03)00163-9.

Moesgaard, L., Reinholdt, P., Nielsen, C.U., Kongsted, J., 2022. Mechanism behind polysorbates' inhibitory effect on P-glycoprotein. Mol. Pharm. 19, 2248–2253. https://doi.org/10.1021/acs.molpharmaceut.2c00074.

Mulet-Cabero, A.-I., Egger, L., Portmann, R., Ménard, O., Marze, S., Minekus, M., Le Feunteun, S., Sarkar, A., Grundy, M.M.L., Carrière, F., Golding, M., Dupont, D., Recio, I., Brodkorb, A., Mackie, A., 2020. A standardised semi-dynamic in vitro digestion method suitable for food – An international consensus. Food Funct. 11, 1702–1720. https://doi.org/10.1039/C9FO01293A.

Nielsen, C.U., Abdulhussein, A.A., Colak, D., Holm, R., 2016. Polysorbate 20 increases oral absorption of digoxin in wild-type Sprague Dawley rats, but not in mdr1a(-/-) Sprague Dawley rats. Int. J. Pharm. 513, 78–87. https://doi.org/10.1016/j.ijpharm.2016.09.011.

Rege, B.D., Kao, J.P.Y., Polli, J.E., 2002. Effects of nonionic surfactants on membrane transporters in Caco-2 cell monolayers. Eur. J. Pharm. Sci. 16, 237–246. https://doi.org/10.1016/S0928-0987(02)00055-6.

Shen, Q., Lin, Y., Handa, T., Doi, M., Sugie, M., Wakayama, K., Okada, N., Fujita, T., Yamamoto, A., 2006. Modulation of intestinal P-glycoprotein function by polyethylene glycols and their derivatives by in vitro transport and in situ absorption studies. Int. J. Pharm. 313, 49–56. https://doi.org/10.1016/j.ijpharm.2006.01.020.

SigmaAldrich, 2023. Cremophor® EL. Accessed 01-03-2024, https://www.sigmaaldrich.com/DK/en/product/mm/238470.

Tomlinson, A., Demeule, B., Lin, B., Yadav, S., 2015. Polysorbate 20 degradation in biopharmaceutical formulations: Quantification of free fatty acids, characterization of particulates, and insights into the degradation mechanism. Mol. Pharm. 12, 3805–3815. https://doi.org/10.1021/acs.molpharmaceut.5b00311.

Yu, H., Hu, Y.Q., Ip, F.C., Zuo, Z., Han, Y.F., Ip, N.Y., 2011. Intestinal transport of bis(12)-hupyridone in Caco-2 cells and its improved permeability by the surfactant Brij-35. Biopharm. Drug. Dispos. 32, 140–150. https://doi.org/10.1002/bdd.745.

Zhang, H., Yao, M., Morrison, R.A., Chong, S., 2003. Commonly used surfactant, Tween 80, improves absorption of P-glycoprotein substrate, digoxin, in rats. Arch. Pharmacal Res. 26, 768–772. https://doi.org/10.1007/bf02976689.